

LA-3324-MS

LA-3324-MS

D3

LOS ALAMOS SCIENTIFIC LABORATORY
of the
University of California
LOS ALAMOS • NEW MEXICO

HASTI

**A Numerical Calculation of Two-Dimensional
Lagrangian Hydrodynamics Utilizing the Concept
of Space-Dependent Time Steps**

DISTRIBUTION STATEMENT A
Approved for Public Release
Distribution Unlimited

Lovelace Foundation - Document Library
Aerospace Medicine and Bioastronautics

UNITED STATES
ATOMIC ENERGY COMMISSION
CONTRACT W-7405-ENG.

Reproduced From
Best Available Copy

DTIC QUALITY INSPECTED

20000915 051

LEGAL NOTICE

This report was prepared as an account of Government sponsored work. Neither the United States, nor the Commission, nor any person acting on behalf of the Commission:

A. Makes any warranty or representation, expressed or implied, with respect to the accuracy, completeness, or usefulness of the information contained in this report, or that the use of any information, apparatus, method, or process disclosed in this report may not infringe privately owned rights; or

B. Assumes any liabilities with respect to the use of, or for damages resulting from the use of any information, apparatus, method, or process disclosed in this report.

As used in the above, "person acting on behalf of the Commission" includes any employee or contractor of the Commission, or employee of such contractor, to the extent that such employee or contractor of the Commission, or employee of such contractor prepares, disseminates, or provides access to, any information pursuant to his employment or contract with the Commission, or his employment with such contractor.

All LA...MS reports are informal documents, usually prepared for a special purpose and primarily prepared for use within the Laboratory rather than for general distribution. This report has not been edited, reviewed, or verified for accuracy. All LA...MS reports express the views of the authors as of the time they were written and do not necessarily reflect the opinions of the Los Alamos Scientific Laboratory or the final opinion of the authors on the subject.

Printed in USA. Price \$2.00. Available from the Clearinghouse for Federal Scientific and Technical Information, National Bureau of Standards, United States Department of Commerce, Springfield, Virginia

**LOS ALAMOS SCIENTIFIC LABORATORY
of the
University of California**

Report written: May 5, 1965

Report distributed: September 2, 1965

HASTI

**A Numerical Calculation of Two-Dimensional
Lagrangian Hydrodynamics Utilizing the Concept
of Space-Dependent Time Steps**

by

Phillip L. Browne and Martha S. Hoyt

ABSTRACT

A numerical experiment is described in which an attempt was made to reduce the calculation time of a two-dimensional, Lagrangian, hydrodynamics code, without loss of accuracy. The reduction was accomplished by utilizing a space-dependent time step; i.e., the frequency with which a point is calculated depends on the rate at which changes are occurring in the vicinity of the point. This system permitted savings to be made by eliminating calculations in regions undergoing relatively slow changes.

ACKNOWLEDGEMENTS

We thank S. R. Orr for his cooperation in explaining many aspects of the Magee code. We also thank K. B. Wallick for making available his knowledge and experience with a Magee-type code, and for his patience in running the comparison problems that were used as standards for judging the accuracy of HASTI. There are many others who helped in other ways. The detailed planning, programming, and problem running were all done by Martha S. Hoyt.

TABLE OF CONTENTS

	<u>Page</u>
Abstract	3
Acknowledgements	3
I. INTRODUCTION	7
II. A BRIEF DESCRIPTION OF THE MAGEE CODE (NON-SPACE-DEPENDENT TIME INTERVAL)	8
A. The Variables	9
B. The Difference Equations	10
III. THE HASTI CODE: GENERAL DESCRIPTION	16
IV. THE FIRST PASS	21
A. The Circle (o) Points	21
B. The Dot (•) Points	23
C. The x Points	23
V. THE SECOND PASS	24
VI. RESULTS	25
VII. CONCLUSIONS	26
REFERENCES	27

I. INTRODUCTION

In many numerical models approximating physical or mathematical systems where successive approximations are used to describe model changes as the calculation proceeds, there are often regions in which changes are taking place more rapidly than in others. The usual computing procedure is to extrapolate all regions of the system at the interval required by the region of most rapid change, resulting in unnecessary calculations for regions undergoing slow changes. It was the purpose of this program to see if eliminating these superfluous calculations might save calculation time, with little loss in accuracy. The disadvantages inherent in such a procedure are the additional storage required and the increased complexity of the code logic, neither of which turns out to be serious in practice, especially when a modern computer with a large memory is used.

Because numerical calculation of two-dimensional hydrodynamics is time-consuming and relatively complicated, and because the authors are somewhat familiar with two-dimensional, Lagrangian hydrodynamics, this field was chosen for experimentation. It was decided to experiment with a Magee-type code inasmuch as it had been studied in some detail by one of the authors and his coworkers.¹ The Magee code was initiated at Los Alamos by H. Kolsky,² and has been developed, improved, and used extensively by S. R. Orr³ and others. It is appropriate to mention here that some other work using a space-dependent time interval has been done by Goad,⁴ using other methods in the code WAT with good success.

The concept of a space-dependent time step can easily be applied to one-dimensional hydrodynamics problems; and the authors feel, with some conviction, that the same approach can be used with problems in-

volving heat or radiation diffusion, in either one or two dimensions. It is possible to speculate further and suggest that similar schemes be used in numerical systems wherever successive approximations are used.

II. A BRIEF DESCRIPTION OF THE MAGEE CODE (NON-SPACE-DEPENDENT TIME INTERVAL)

Consider a physical system of cylindrical symmetry, which is represented in a cylindrical (r,z) coordinate system by a mesh consisting of quadrilateral zones (as shown in Fig. 1), rotated through an angle of one radian about the z axis. (The use of this angle simplifies the formulae and calculations by eliminating the factor 2π .) Thus, each quadrilateral zone represents an element of volume. Because of the cylindrical symmetry, all quantities are dependent only on r and z . Inasmuch as the Lagrangian viewpoint has been adopted, the mesh is considered to be imbedded in and to move with the fluid.

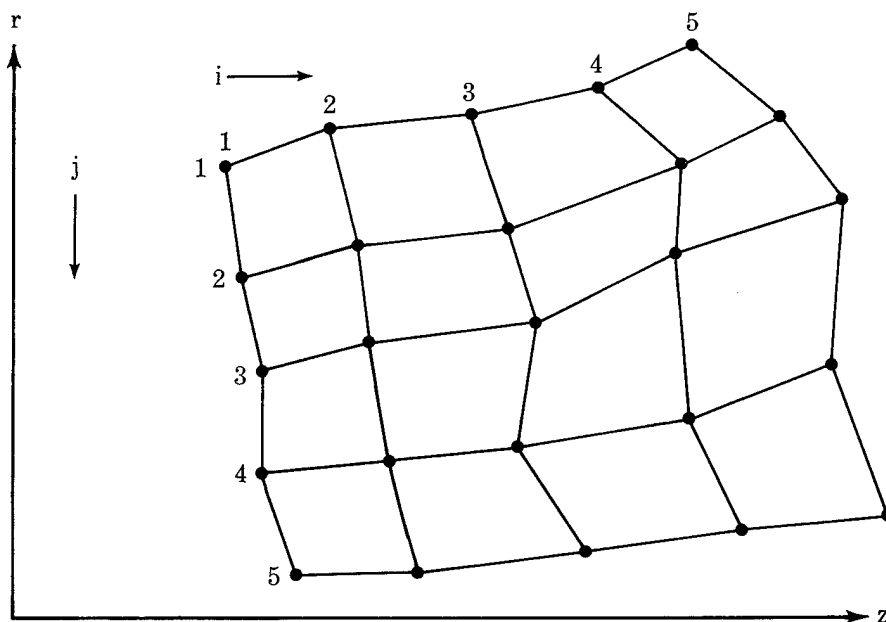


Fig. 1. A Typical Magee Mesh

In order to describe a hydrodynamic system mathematically, it is necessary to use the principles of conservation of mass, momentum, and energy, together with an equation of state relating the thermodynamic quantities. Also, it is necessary to know the initial condition of the system and some boundary conditions as the hydrodynamic activity unfolds. In the following paragraphs, the required variables and difference-approximations of these equations will be enumerated.

IIA. The Variables

In Magee, many of the quantities are assumed to be associated with the points (the intersections of grid lines) and are identified by a pair of integers, (i,j), as subscripts, i.e.:

$$\left. \begin{array}{l} \text{The coordinates of a point, } (r_{i,j} \text{ and } z_{i,j}) \\ \text{The velocity components of a point, } (\dot{r}_{i,j} \text{ and } \dot{z}_{i,j}) \\ \text{The acceleration components of a point, } (\ddot{r}_{i,j} \text{ and } \ddot{z}_{i,j}) \end{array} \right\} (1)$$

Other quantities are assumed to be associated with the zones and are identified by a pair of fractional subscripts, $(i-\frac{1}{2}, j-\frac{1}{2})$, i.e.:

$$\left. \begin{array}{l} \text{The pressure and Richtmyer-Von Neumann artificial dissipative} \\ \text{term,}^{5,6} (p+q)_{i-\frac{1}{2}, j-\frac{1}{2}} = P_{i-\frac{1}{2}, j-\frac{1}{2}} \\ \text{The internal energy per unit original volume, } \epsilon_{i-\frac{1}{2}, j-\frac{1}{2}} \\ \text{The mass, density, and relative volume, } m_{i-\frac{1}{2}, j-\frac{1}{2}}, \\ \rho_{i-\frac{1}{2}, j-\frac{1}{2}}, V_{i-\frac{1}{2}, j-\frac{1}{2}} \\ \text{The stability number, } (w/b)_{i-\frac{1}{2}, j-\frac{1}{2}}^2 \end{array} \right\} (2)$$

The times, t , $t+\Delta t$, $t+\Delta t/2$, at which quantities are assumed to be known or calculated are identified by superscripts such as n , $n+1$ and $n+\frac{1}{2}$. The superscript $n+\frac{1}{2}$ is also used to identify the change in a

quantity between t^n , t^{n+1} . The superscript 0 denotes the initial value of a quantity at the start of the problem.

IIB. The Difference Equations

The conservation of mass is not expressed explicitly in a separate equation; but, rather, it is assumed implicitly in writing the momentum and energy equations. Because the internal energy equation is applied to a zone as an entity, for that equation the mass of each zone is assumed to be conserved. And, because the momentum equation is applied to a point as an entity, for that equation the masses associated with each point are considered to be always the same (specifically, one-fourth of the mass of each of the adjacent zones).

To simplify this discussion, the difference equations will be listed in a plausible sequence for calculation, not necessarily the sequence actually used in Magee (in which a number of variations have been tried). Several passes through the mesh might be required to perform the calculations as presented here.

Assume that all calculations have been performed up through cycle n ($t=t^n$), so that for all points and zones there are available the values of:

$$r^n, z^n, \dot{r}^{n-\frac{1}{2}}, \dot{z}^{n-\frac{1}{2}}, V^n, P^n, \text{ and } \epsilon^n \quad (3)$$

The accelerations at time, n , are calculated from an approximation^{1,3} of the law of conservation of momentum given in Eq. (4). The arguments used to derive these equations are too lengthy to be given here, but will hopefully be derived in a subsequent report. The quantities used in Eq. (4) are associated with a group of points and zones as shown in Fig. 2.

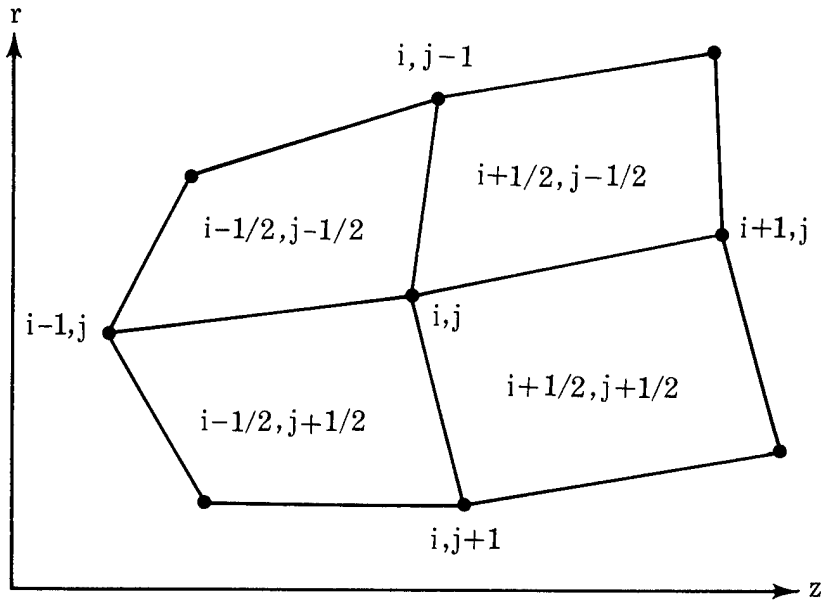


Fig. 2. A Typical Magee Point, (i, j) , with the Adjacent Zones and Points, Illustrating the Notation Used in Eq. (4), below.

$$\begin{aligned}
 \ddot{r}_{i,j}^n = & \frac{1}{4} \left\{ \frac{(P_{i-\frac{1}{2}, j-\frac{1}{2}}^n - P_{i+\frac{1}{2}, j-\frac{1}{2}}^n)(z_{i,j}^n - z_{i, j-1}^n) \frac{1}{2}(r_{i,j}^n + r_{i, j-1}^n)}{\frac{1}{4}(m_{i-\frac{1}{2}, j-\frac{1}{2}}^0 + m_{i+\frac{1}{2}, j-\frac{1}{2}}^0)} \right. \\
 & + \frac{(P_{i+\frac{1}{2}, j-\frac{1}{2}}^n - P_{i+\frac{1}{2}, j+\frac{1}{2}}^n)(z_{i,j}^n - z_{i+1, j}^n) \frac{1}{2}(r_{i,j}^n + r_{i+1, j}^n)}{\frac{1}{4}(m_{i+\frac{1}{2}, j-\frac{1}{2}}^0 + m_{i+\frac{1}{2}, j+\frac{1}{2}}^0)} \\
 & + \frac{(P_{i+\frac{1}{2}, j+\frac{1}{2}}^n - P_{i-\frac{1}{2}, j+\frac{1}{2}}^n)(z_{i,j}^n - z_{i, j+1}^n) \frac{1}{2}(r_{i,j}^n + r_{i, j+1}^n)}{\frac{1}{4}(m_{i+\frac{1}{2}, j+\frac{1}{2}}^0 + m_{i-\frac{1}{2}, j+\frac{1}{2}}^0)} \\
 & \left. + \frac{(P_{i-\frac{1}{2}, j+\frac{1}{2}}^n - P_{i-\frac{1}{2}, j-\frac{1}{2}}^n)(z_{i,j}^n - z_{i-1, j}^n) \frac{1}{2}(r_{i,j}^n + r_{i-1, j}^n)}{\frac{1}{4}(m_{i-\frac{1}{2}, j+\frac{1}{2}}^0 + m_{i-\frac{1}{2}, j-\frac{1}{2}}^0)} \right\}
 \end{aligned}$$

$$\begin{aligned}
\ddot{z}_{i,j}^n = \frac{1}{4} & \left\{ \frac{(P_{i-\frac{1}{2},j-\frac{1}{2}}^n - P_{i+\frac{1}{2},j-\frac{1}{2}}^n)(r_{i,j-1}^n - r_{i,j}^n) \frac{1}{2}(r_{i,j-1}^n + r_{i,j}^n)}{\frac{1}{4}(m_{i-\frac{1}{2},j-\frac{1}{2}}^0 + m_{i+\frac{1}{2},j-\frac{1}{2}}^0)} \right. \\
& + \frac{(P_{i+\frac{1}{2},j-\frac{1}{2}}^n - P_{i+\frac{1}{2},j+\frac{1}{2}}^n)(r_{i+1,j}^n - r_{i,j}^n) \frac{1}{2}(r_{i+1,j}^n + r_{i,j}^n)}{\frac{1}{4}(m_{i+\frac{1}{2},j-\frac{1}{2}}^0 + m_{i+\frac{1}{2},j+\frac{1}{2}}^0)} \\
& + \frac{(P_{i+\frac{1}{2},j+\frac{1}{2}}^n - P_{i-\frac{1}{2},j+\frac{1}{2}}^n)(r_{i,j+1}^n - r_{i,j}^n) \frac{1}{2}(r_{i,j+1}^n + r_{i,j}^n)}{\frac{1}{4}(m_{i+\frac{1}{2},j+\frac{1}{2}}^0 + m_{i-\frac{1}{2},j+\frac{1}{2}}^0)} \\
& \left. + \frac{(P_{i-\frac{1}{2},j+\frac{1}{2}}^n - P_{i-\frac{1}{2},j-\frac{1}{2}}^n)(r_{i-1,j}^n - r_{i,j}^n) \frac{1}{2}(r_{i-1,j}^n + r_{i,j}^n)}{\frac{1}{4}(m_{i-\frac{1}{2},j+\frac{1}{2}}^0 + m_{i-\frac{1}{2},j-\frac{1}{2}}^0)} \right\} \quad (4)
\end{aligned}$$

These accelerations may now be used to advance the velocities of all points to time, $n+\frac{1}{2}$, by

$$\begin{aligned}
\dot{r}^{n+\frac{1}{2}} &= \dot{r}^{n-\frac{1}{2}} + \dot{r}^n \left[\frac{1}{2}(t^{n+1} + t^n) - \frac{1}{2}(t^n + t^{n-1}) \right] \\
\dot{z}^{n+\frac{1}{2}} &= \dot{z}^{n-\frac{1}{2}} + \dot{z}^n \left[\frac{1}{2}(t^{n+1} + t^n) - \frac{1}{2}(t^n + t^{n-1}) \right] \quad (5)
\end{aligned}$$

Then, these velocities are used to advance the coordinates of all points to time, $n+1$, by

$$\begin{aligned}
r^{n+1} &= r^n + \dot{r}^{n+\frac{1}{2}} \Delta t^{n+\frac{1}{2}} \\
z^{n+1} &= z^n + \dot{z}^{n+\frac{1}{2}} \Delta t^{n+\frac{1}{2}}
\end{aligned} \quad (6)$$

where

$$\Delta t^{n+\frac{1}{2}} = t^{n+1} - t^n$$

The next steps involve the calculation of V , P , ϵ , etc., for the zones at time, $n+1$.

The actual volume v_{\square} of a quadrilateral zone can be calculated exactly as the sum of the volumes of two zones of triangular cross section (see Fig. 3).

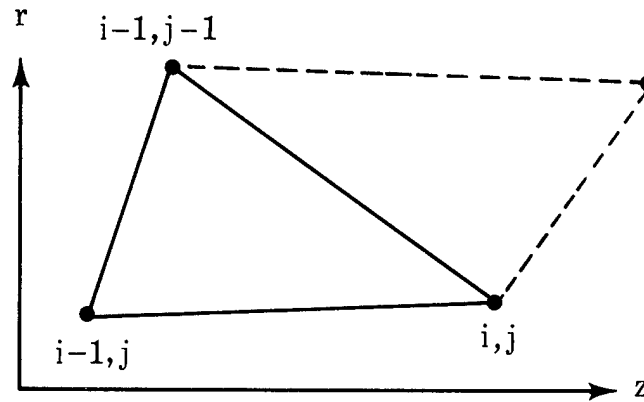


Fig. 3. The Two Triangular Zones Making up a Quadrilateral Zone

The volume v_{Δ} of a triangular zone is given by

$$v_{\Delta} = A_{\Delta} \bar{r}_{\Delta} \quad (7)$$

where

$$A_{\Delta} = \frac{1}{2} \begin{vmatrix} 1 & 1 & 1 \\ r_{i-1,j-1} & r_{i,j} & r_{i-1,j} \\ z_{i-1,j-1} & z_{i,j} & z_{i-1,j} \end{vmatrix} \quad (8)$$

and

$$\begin{aligned} \bar{r}_{\Delta} &= \text{centroid of the triangle} \\ &= \frac{1}{3}(r_{i-1,j-1} + r_{i,j} + r_{i-1,j}) \end{aligned} \quad (9)$$

For each quadrilateral zone, the relative volume is then obtained from

$$V_{\square}^{n+1} = V_{\square}^{n+1} / V_{\square}^0 \quad (10)$$

the V_{\square}^0 having been obtained at the start of the problem in order to calculate the masses of the zones by

$$m_{\square}^0 = \rho_{\square}^0 V_{\square}^0 \quad (11)$$

These masses, assumed to be constant in time, have been used in Eq. (4). If, at any time, the density of a zone is required, it is obtained by

$$\rho_{\square}^{n+1} = \frac{m_{\square}^0}{V_{\square}^{n+1}} = \frac{m_{\square}^0}{V_{\square}^{n+1} V_{\square}^0} \quad (12)$$

The Richtmyer-Von Neumann artificial dissipative term^{5,6} is calculated from the rate of volume change for each zone by

$$q^{n+1} = (1.2)^2 \rho_0 A^{n+1} \frac{1}{(V^{n+1})^2} \left(\frac{\Delta V^{n+1/2}}{\Delta t^{n+1/2}} \right)^2 \quad (13)$$

where

$$\Delta V^{n+1/2} = V^{n+1} - V^n < 0, \text{ and}$$

$$A^{n+1} = \text{area of quadrilateral at time, } n+1.$$

In the case of a zone expansion, i.e., $\Delta V^{n+1/2} > 0$,

$$q^{n+1} = 0 \quad (13a)$$

The pressure, p , and internal energy, ϵ , of each zone are obtained from the equation of state

$$p^{n+1} = p(V^{n+1}, \epsilon^{n+1}) \quad (14)$$

and from the equation of conservation of energy, $d\epsilon = -PdV$, in difference form,

$$\epsilon^{n+1} = \epsilon^n - \frac{1}{2}(P^n + p^{n+1} + q^{n+1})\Delta V^{n+1/2} \quad (15)$$

If (14) and (15) cannot be solved simultaneously for the two unknowns, p^{n+1} and ϵ^{n+1} , then iterative techniques are used.

The White stability number for each zone is calculated by⁷

$$\left[\left(\frac{w}{1.2} \right)^2 \right]^{n+1} = \frac{1 + 3P^{n+1}V^{n+1}}{\rho_0 A^{n+1}} \left(\frac{\Delta t^{n+1/2}}{1.2} \right)^2 + 4 \left| \frac{\Delta V^{n+1/2}}{V^{n+1}} \right| \quad (16)$$

and the time interval, $\Delta t^{n+3/2}$, to be used for the next cycle is chosen so that the maximum of the stability numbers for all the zones with

$$\Delta t^{n+3/2} \rightarrow \Delta t^{n+1/2}$$

satisfies

$$0.035 < \left(\frac{w}{1.2} \right)_{\max}^2 < 0.14 \quad (17)$$

or

$$0.2245 < w_{\max} < 0.45$$

Frequent calculation of the total energies in regions of a problem are useful, although not necessary. The internal energy is added by zones

$$(\text{IE})^n = \sum_{i,j} \epsilon_{i-1/2, j-1/2}^n U_{i-1/2, j-1/2}^0 \quad (18)$$

and the kinetic energy is added by points

$$\begin{aligned}
 (KE)^n = \sum_{i,j} [& (\dot{r}_{i,j}^n)^2 + (\dot{z}_{i,j}^n)^2] [\frac{m_{i-\frac{1}{2},j-\frac{1}{2}}^0}{4} + \frac{m_{i-\frac{1}{2},j+\frac{1}{2}}^0}{4} \\
 & + \frac{m_{i+\frac{1}{2},j-\frac{1}{2}}^0}{4} + \frac{m_{i+\frac{1}{2},j+\frac{1}{2}}^0}{4}] \quad (19)
 \end{aligned}$$

III. THE HASTI CODE: GENERAL DESCRIPTION

Because the HASTI code was experimental, emphasis was placed on achieving a code that would work properly and accurately, yet be convenient to change. Less attention was given to conserving storage and machine time by the use of short cuts and clever manipulation. Consequently, there may be instances where the code is inefficient in these respects.

In any problem, the points of the mesh can be classified into regions, or groups, according to the maximum time intervals at which the quantities in those regions may be calculated without producing instability or inaccuracy. Goad⁴ has used a method of listing points in a set of tables. We have chosen a different method, in which two time values are stored at the end of a cycle for each point:

$$\begin{aligned}
 t_{i,j}^n &= \text{last time at which the point was calculated} \\
 t_{i,j}^{n+1} &= \text{next time at which the point should be calculated} \quad (20)
 \end{aligned}$$

There is also available a time

$$t_{\min}^{n+1} = \text{minimum of all } t_{i,j}^{n+1} \quad (21)$$

which is the next time a calculation must be made for some points in the problem. Furthermore, there is stored a time

$$t_{\text{major}}^{n+1} = \text{next time at which all points must be calculated} \quad (22)$$

The purpose of this time is to bring the calculation together for analysis (pointing, plotting, etc.), and its choice is arbitrary. Variations in time intervals were made by powers of two.

For each point, i, j , among the quantities stored are:*

$$\left. \begin{array}{ll} r_{i,j}^n & \text{representing } r_{i,j}, z_{i,j} \text{ at } t_{i,j}^n \\ v_{i,j}^{n+\frac{1}{2}} & \text{representing } \dot{r}_{i,j}, \dot{z}_{i,j} \text{ at } \frac{1}{2}(t_{i,j}^n + t_{i,j}^{n+1}) \\ a_{i,j}^n & \text{representing } \ddot{r}_{i,j}, \ddot{z}_{i,j} \text{ at } t_{i,j}^n \\ V_{i-\frac{1}{2},j-\frac{1}{2}}^n & \text{representing } V_{i-\frac{1}{2},j-\frac{1}{2}}, P_{i-\frac{1}{2},j-\frac{1}{2}}, \epsilon_{i-\frac{1}{2},j-\frac{1}{2}} \text{ at } t_{i,j}^n \\ \Delta t_{i-\frac{1}{2},j-\frac{1}{2}}^+ & \text{representing the next time interval allowed by} \\ & \text{the stability number} \end{array} \right\} (23)$$

To illustrate the method, consider the problem to be at the stage where, in the logical mesh, there is one region of points (denoted • in Fig. 4) for which $t^{n+1} = t_{\text{min}}^{n+1}$. All other points have $t^{n+1} > t_{\text{min}}^{n+1}$. The values of t^n for points may differ. The authors believe that the arguments and methods to be presented also apply to cases where there are many such regions and/or regions of more complex shapes. And, indeed, the problems run with the code have turned up no exceptions to this theory.

Because the • points are probably in a region undergoing more rapid changes than the surrounding points, this rapidly changing domain is enclosed by a "buffer region", one zone thick (denoted by the shaded area in Fig. 4). Enough calculations are made for the buffer region so that the stability number can be calculated for these zones in order to alert the code if the disturbance is moving into the buffer region. buffer zone in Fig. 4 is delineated by three kinds of x points ($\nwarrow x$, $\uparrow x$, $\leftarrow x$)

*For simplification of notation in the subsequent discussion and flow diagrams, several quantities will be represented by the same symbol.

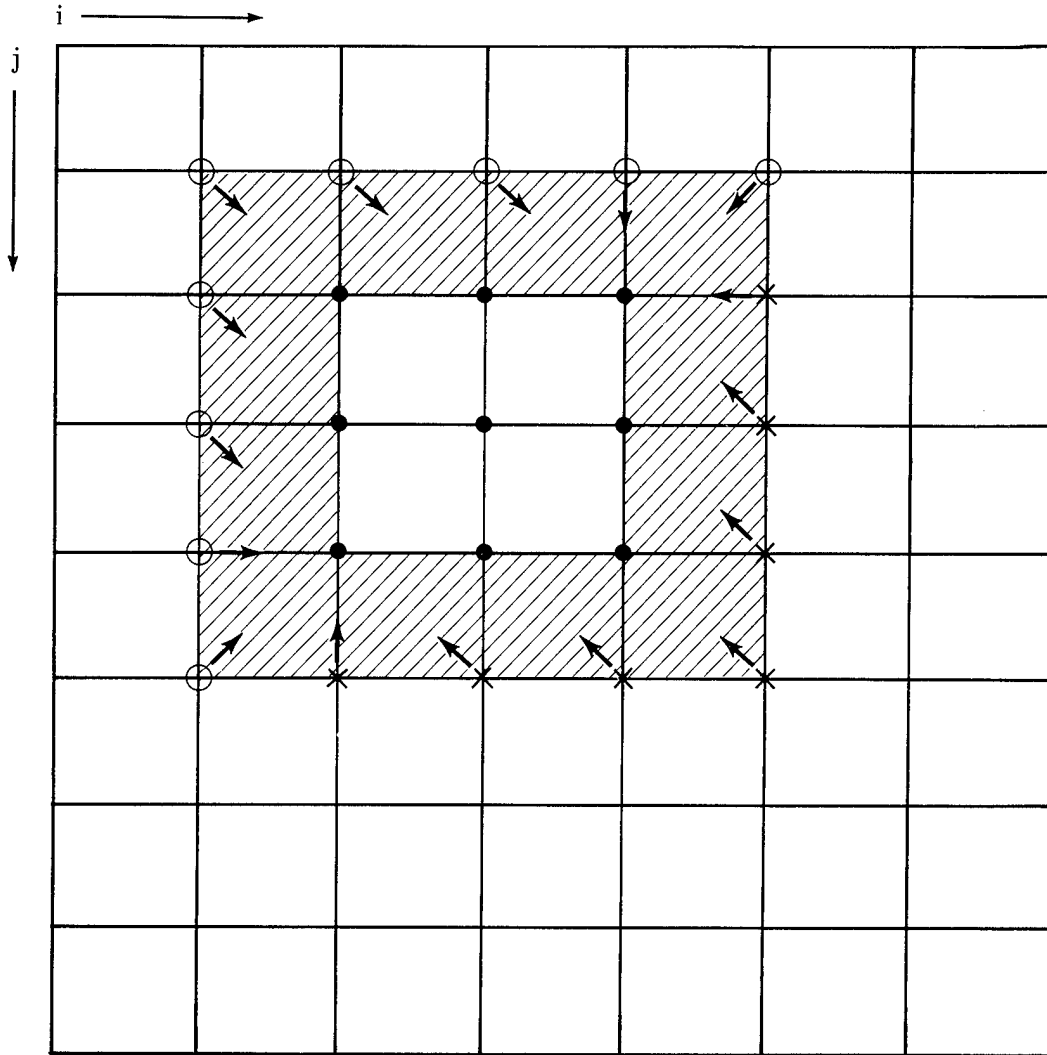


Fig. 4. A Simple HASTI Logical Mesh, Showing the Various Types of •, x, and o Points

and by five kinds of o points ($o_v, o_p, o_{\rightarrow}, o_{\rho}, o^{\prime}$) all of which are defined by a succession of tests on t^{n+1} , as shown in the flow diagram (Fig. 5).

In order to have the required quantities available at the proper time, the code makes two passes through the mesh, taking points in the order

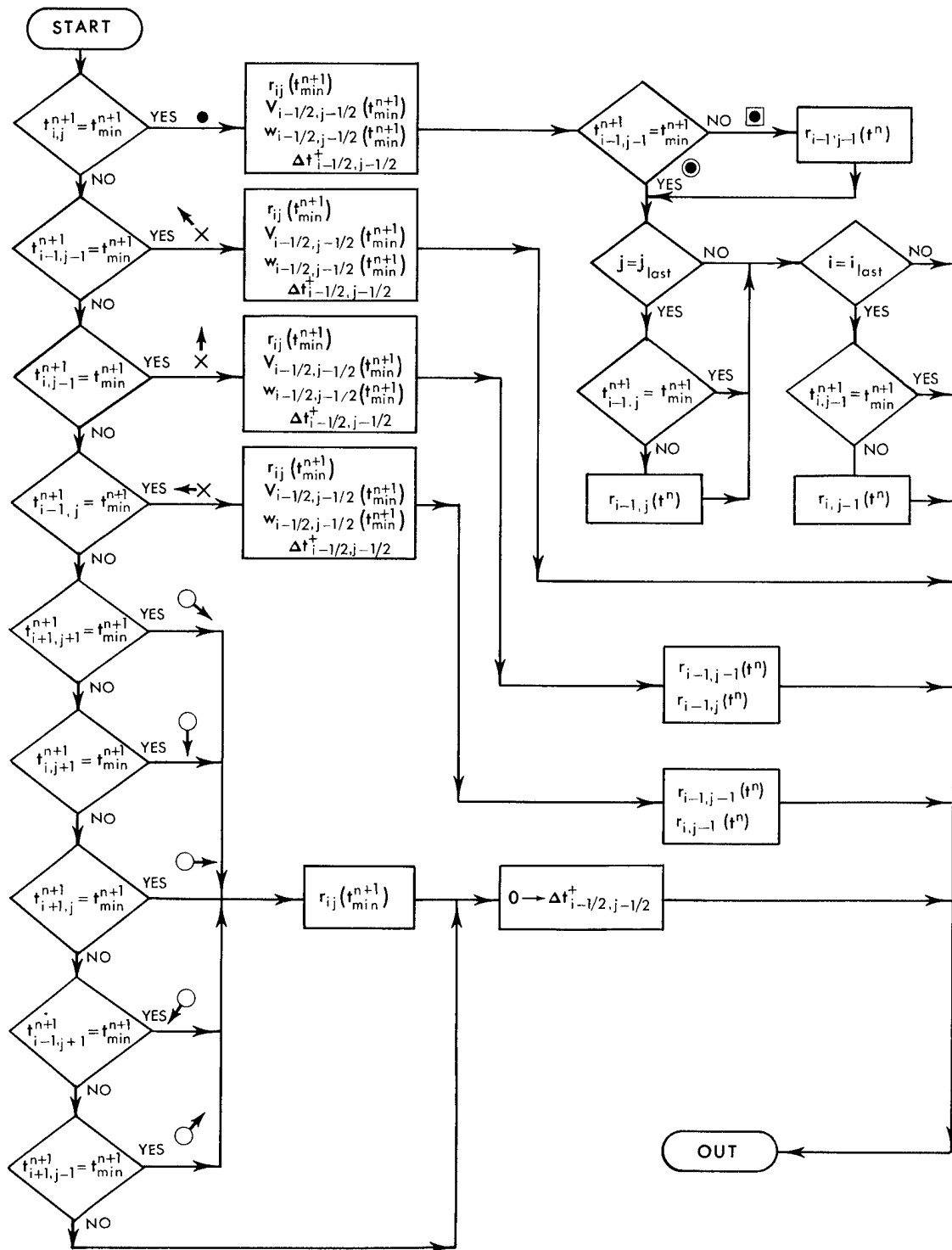


Fig. 5. HASTI - First Pass-Through Mesh

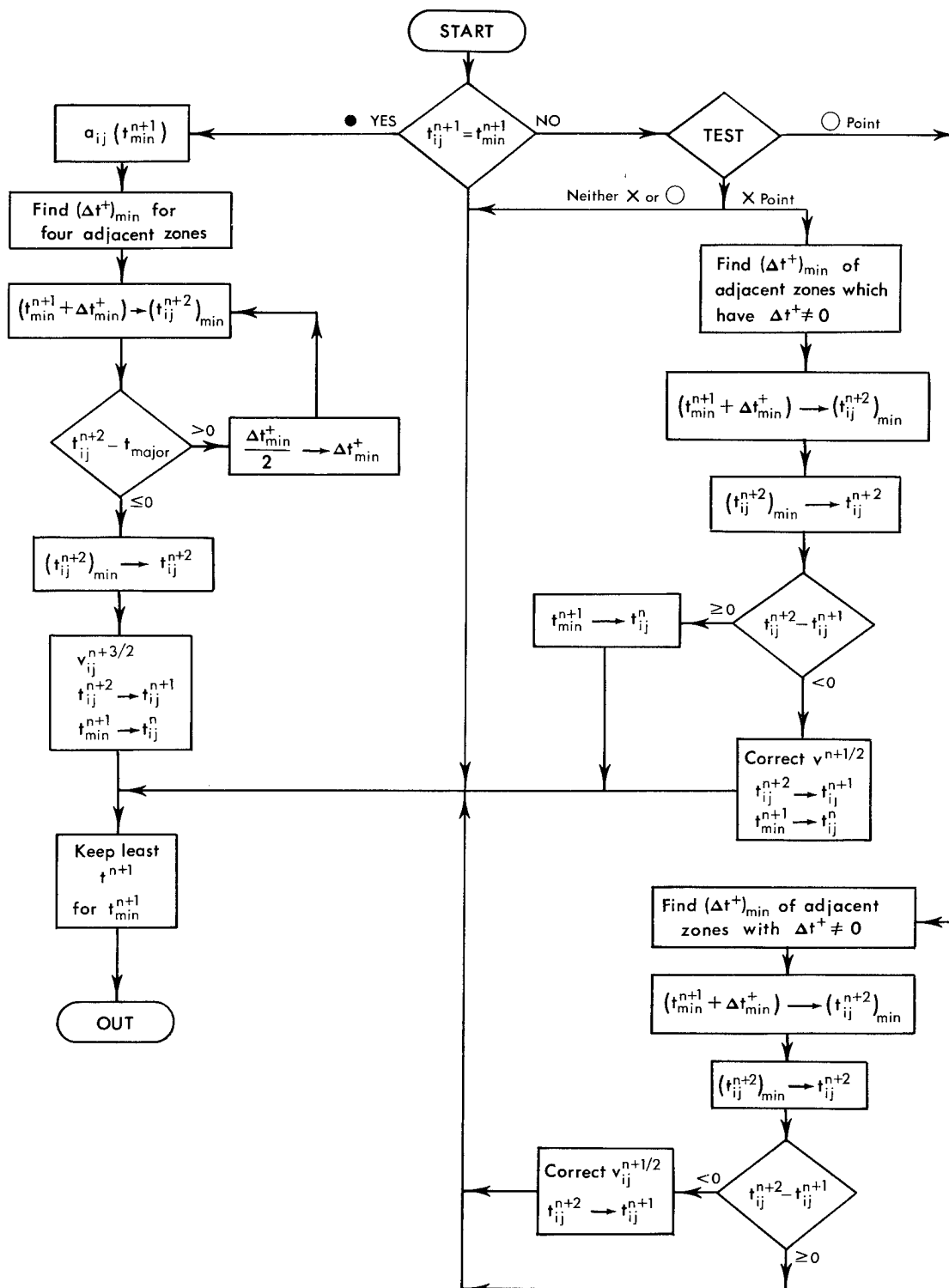


Fig. 6. HASTI - Second Pass-Through Mesh

$$\begin{array}{l}
i = 1, j = 1, 2, \dots, j_{\text{last}} \\
i = 2, j = 1, 2, \dots, j_{\text{last}} \\
\dots\dots\dots \\
i = i_{\text{last}}, j = 1, 2, \dots, j_{\text{last}}
\end{array}
\left. \vphantom{\begin{array}{l} i = 1, j = 1, 2, \dots, j_{\text{last}} \\ i = 2, j = 1, 2, \dots, j_{\text{last}} \\ \dots\dots\dots \\ i = i_{\text{last}}, j = 1, 2, \dots, j_{\text{last}} \end{array}} \right\} (24)$$

On the first pass (see Fig. 5) calculations are made for

$$r^{n+1}, v^{n+1}, w^{n+1}, \text{ and } \Delta t^+ \quad (25)$$

while on the second pass (see Fig. 6), the quantities determined are

$$a^{n+1}, v^{n+3/2}, \text{ revised } t^n, \text{ and } t^{n+1} \quad (26)$$

Because of space limitations, the flow diagrams do not include the equations used for calculations; these equations are part of the discussion of the problem illustrated in Fig. 4.

IV. THE FIRST PASS

As the calculation proceeds on the first pass through the mesh of the example in Fig. 4 [following the ordering scheme shown in Eq. (24)], circle (o) points, dot (•) points, and x points will be encountered. The first pass is used to calculate the coordinates and thermodynamic quantities.

IVA. The Circle (o) Points

In the example in Fig. 4, the first points in the mesh requiring calculation are the circle (o) points. The coordinates of these points must be advanced to t_{min}^{n+1} because this information is required to obtain accurate volumes, V , for the adjacent dot (•) points. Failure to advance the circle (o) points can and has resulted in the undesirable effect of an associated zone apparently compressing when, actually, it

is expanding, thereby producing an artificial viscosity by Eq. (13) when there should be none. Such a fictitiously produced perturbation has a tendency to spread through the mesh in the form of oscillations of points about their proper positions, and may result in instability if the stability condition is not made more severe.

Consider the pictorial time scale of Fig. 7, in which the times for a dot point are represented below the line by t^n and t_{\min}^{n+1} ; and the times for an adjacent circle point are represented above the line by $(t')^n$ and $(t')^{n+1}$.

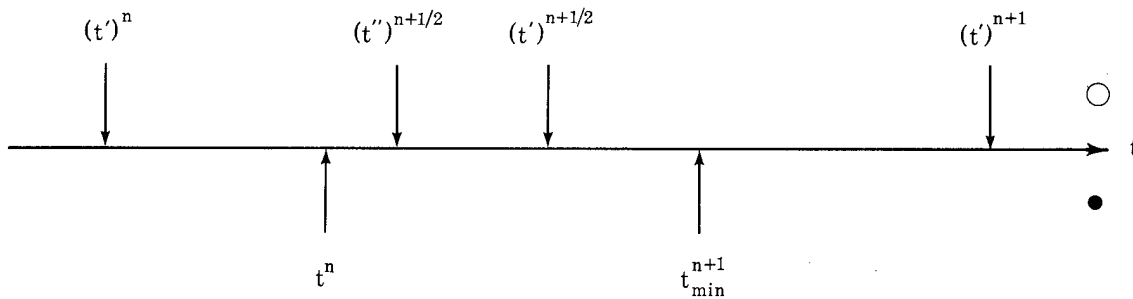


Fig. 7. A Pictorial Time Scale for Adjacent Circle and Dot Points

The coordinates, r^n , and accelerations, a^n , of the circle point are known at $(t')^n$; the velocities, $v^{n+\frac{1}{2}}$, are known at $(t')^{n+\frac{1}{2}} = \frac{1}{2}[(t')^n + (t')^{n+1}]$; and it is desired to advance the coordinates to t_{\min}^{n+1} . The simplest way to do this is to assume that $v^{n+\frac{1}{2}}$ is valid for the whole interval from $(t')^n$ to $(t')^{n+1}$ and, hence, by Eq. (6):

$$r(t_{\min}^{n+1}) = r^n + v^{n+\frac{1}{2}}[t_{\min}^{n+1} - (t')^n] \quad (27)$$

If more accuracy is desired, the velocity can be adjusted from $(t')^{n+\frac{1}{2}}$ to $(t'')^{n+\frac{1}{2}} = \frac{1}{2}[(t')^n + t_{\min}^{n+1}]$ by an equation similar to Eq. (5):

$$(v'')^{n+\frac{1}{2}} = v^{n+\frac{1}{2}} + a^n [(t'')^{n+\frac{1}{2}} - (t')^{n+\frac{1}{2}}] \quad (28)$$

before using Eq. (27).

Once $r(t_{\min}^{n+1})$ has been used to calculate the related volumes, it is then deadvanced to r^n by Eq. (27); and the velocity is corrected back to $v^{n+\frac{1}{2}}$ by Eq. (28), so that the proper values are in storage for the two times $(t')^n$ and $(t')^{n+1}$ still associated with that point. In order to delay the corrections until after the volumes have been calculated, the corrections are made after other x or dot points, further along in the mesh, have been calculated (see Fig. 5). The delay is necessary in order to have the coordinates of all corners of a zone at t_{\min}^{n+1} , so that the volume can be calculated more accurately.

IVB. The Dot (•) Points

Calculations for the dot (•) points are quite straightforward. Knowing t^n , t_{\min}^{n+1} , a^n , and v^n , one uses Eq. (6) to compute

$$r(t_{\min}^{n+1}) = r^n + v^{n+\frac{1}{2}}(t_{\min}^{n+1} - t^n) \quad (29)$$

and, subsequently, to compute $V(t_{\min}^{n+1})$, $w(t_{\min}^{n+1})$, etc. by Eqs. (10), (13), (14), (15) and (16). The Δt^+ is the largest Δt that satisfies Eq. (17). This procedure is equivalent to what is normally described as time-splitting and -doubling.

IVC. The x Points

The x points are buffer points similar to the circle points; but whereas the circle points are deadvanced to their original positions after use, the x points are left in their new positions.

Consider the pictorial time scale in Fig. 8 in which times for a dot point are represented above the line by t^n and t_{\min}^{n+1} ; and the times

for an adjacent x point are represented below the line by $(t')^n$ and $(t')^{n+1}$.

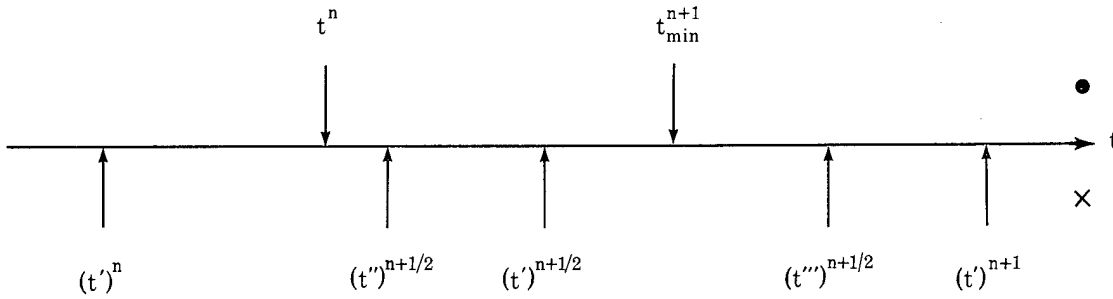


Fig. 8. A Pictorial Time Scale for Adjacent x and • Points

The coordinates, r^n , and accelerations, a^n , of the x point are known at $(t')^n$. The velocities, $v^{n+\frac{1}{2}}$, are known at $(t')^{n+\frac{1}{2}} = \frac{1}{2}[(t')^n + (t')^{n+1}]$; and it is desired to advance the coordinates to t_{\min}^{n+1} . Again, as a first approximation one can use Eq. (27) or, for a better approximation, Eqs. (28) and (27). Now, however, it is desired to retain $r(t_{\min}^{n+1})$, so the velocity must be advanced to $(t''')^{n+\frac{1}{2}} = \frac{1}{2}[t_{\min}^{n+1} + (t')^{n+1}]$ by

$$(v''')^{n+\frac{1}{2}} = (v'')^{n+\frac{1}{2}} + a^n [(t''')^{n+\frac{1}{2}} - (t'')^{n+\frac{1}{2}}] \quad (30)$$

V. THE SECOND PASS

At the start of the second pass, the coordinates and thermodynamic quantities have been calculated for all the necessary points at t_{\min}^{n+1} . During this pass it is necessary to calculate accelerations and velocities, and to analyze the stability number in order to set up a new pair of times, where necessary.

New accelerations at t_{\min}^{n+1} are calculated only for the dot points by Eq. (4). Before new velocities are computed, the times must be analyzed.

For each point, the Δt^+ 's of the four adjacent zones are examined; and the smallest, nonzero Δt^+ is chosen to obtain

$$(t_{i,j}^{n+2})_{\min} = (t_{\min}^{n+1}) + \Delta t_{\min}^+ \quad (31)$$

which is the next time at which that point must be calculated. The point is thus controlled by the adjacent zone in which the most severe stability condition is present. The $(t_{i,j}^{n+2})_{\min}$ value is then compared to t_{major} , and the smaller of the two is chosen as the actual $t_{i,j}^{n+2}$ to be used for the point.

For the dot points, the new velocities are then calculated as in Eq. (5),

$$\begin{aligned} v^{n+3/2} &= v^{n+1/2} + a(t_{\min}^{n+1}) \left[\frac{1}{2}(t_{i,j}^{n+2} + t_{\min}^{n+1}) - \frac{1}{2}(t_{\min}^{n+1} + t_{i,j}^n) \right] \\ &= v^{n+1/2} + a(t_{\min}^{n+1}) \left[\frac{1}{2}(t_{i,j}^{n+2} - t_{i,j}^n) \right] \end{aligned} \quad (32)$$

The remainder of Fig. 6 deals with the shifting of times in storage to prepare for the next cycle.

VI. RESULTS

There is no need to describe in detail the problems used to test the code. Suffice it to say that the problems included a number of one-dimensional systems, such as planes, cylinders, and spheres, in order to insure that HASTI did not affect the symmetry of such systems. Further, several simple problems with real two-dimensional motions were completed. The problems involved a variety of situations involving shocks, rarefactions, free surface motion, sliding motion along a fixed boundary, and fixed boundaries.

In all cases, the coordinates and densities of the problems run by the HASTI code agreed with the problems run by a Magee-like code to within one percent. In accurate tests of machine time used (excluding input-output), the HASTI problems ran two to three times faster than the Magee ones. Because only a limited effort was spent making HASTI an efficient code, while the Magee-type code is very efficient, there is a good possibility of increasing this time-saving factor.

VII. CONCLUSIONS

The time-saving possibilities of a space-dependent time step in the numerical calculation of two-dimensional, Lagrangian hydrodynamics have been illustrated; and a fairly straightforward method has been suggested. The method apparently does not save as much time as the system used by Goad,⁴ but it is felt that further work and experimentation with HASTI could yield greater time savings. If less emphasis were placed on accuracy, (for example, eliminating some of the velocity adjustments in Section IV) and if more emphasis were placed on efficient use of the machine (saving quantities calculated on one point for use with another point), further time savings could result. The method was found to be sufficiently general and flexible so that changes and refinements of the code could be made without too much difficulty. For example, a modified version of the Magee "fudge" was added to stop any point that attempted to cross the diagonal of the zone.

REFERENCES

1. P. L. Browne, and K. B. Wallick, private communication, Los Alamos, 1963-64.
2. H. Kolsky, Los Alamos Scientific Laboratory Report IA-1867, A Method for the Numerical Solution of Transient Hydrodynamic Shock Problems in Two Space Dimensions, April 1955.
3. S. R. Orr, private communication, Los Alamos, 1959-60.
4. W. Goad, Los Alamos Scientific Laboratory Report IAMS-2365, WAT: A Numerical Method for Two-Dimensional Unsteady Flow, November 1960.
5. J. Von Neumann and R. D. Richtmyer, J. Appl. Phys. 21, 232 (1950).
6. R. D. Richtmyer, Difference Methods for Initial Value Problems, Interscience Publishers, Inc., New York, (1957) p. 208.
7. H. Kolsky, Office Memorandum, Los Alamos, June 1962.